PROCEEDINGS OF SCIENCE

η and η' Physics at BESIII

Shuang-shi Fang[*†]

Institue of High Energy Physics, CAS, Beijing, China

E-mail: fangss@ihep.ac.cn

With a sample of 1.3 billion J/ψ events collected with the BESIII detector, the recent results on η/η' decays are presented, including the Dalitz plot analysis of $\eta \to \pi^+\pi^-\pi^0$, $\eta/\eta' \to \pi^0\pi^0\pi^0$, observations of $\eta' \to \gamma e^+e^-$ and $\eta \to \pi^+\pi^-\pi^{+(0)}\pi^{-(0)}$, and the preliminary results on the decay dynamics of $\eta' \to \gamma\pi^+\pi^-$.

The 8th International Workshop on Chiral Dynamics,
June 29 -July 3, 2015
Pisa, Italy

*Speaker.
†On behalf of the BESIII Collaboration

PoS(CD15)032

1. Introduction

At present a sample of 1.31×10^9 J/ψ events was collected at the BESIII detector, which offers an opportunity to study the η/η' decay dynamics. Since η and η' were discovered half a century ago, both of them have been attracted both theoretical and experimental attentions due to their special role in understanding low energy Quantum Chromodynamics (QCD). In particular for η', it is much heavier than the Goldstone bosons of broken chiral symmetry, and it has a special role in hadron physics because of its interpretation as a singlet state arising from the axial $U(1)$ anomaly. Therefore η' decay dynamics remains a subject of extensive theoretical studies aiming at extensions of chiral perturbation theory (ChPT). In this talk, the recent results on η/η' decays via J/ψ radiative decays are presented.

2. Dalitz plot analysis of $\eta \to \pi^+\pi^-\pi^0$ and $\eta/\eta' \to \pi^0\pi^0\pi^0$[1]

Recently considerable theoretical efforts, see *e.g.* [2, 3, 4, 5, 6, 7, 8, 9], have been invested to explain the discrepancy that the predicted decay width of $\eta \to \pi^+\pi^-\pi^0$ [10] at the tree level of ChPT is much lower than the experimental value of 300 ± 11 eV [11]. To distinguish between the different theoretical approaches, precise measurements of the matrix elements for $\eta \to \pi^+\pi^-\pi^0$ and the decay width are needed.

For $\eta \to \pi^+\pi^-\pi^0$ decays, a sample of 8×10^4 $\eta \to \pi^+\pi^-\pi^0$ candidate events are selected and the background contamination is estimated to be about 0.1% as shown in Fig. 1 (a), which is neglected in the extraction of the Dalitz plot parameters. The two the Dalitz plot variables are defined as $X = \frac{\sqrt{3}}{Q}(T_{\pi^+} - T_{\pi^-})$ and $Y = \frac{m_\eta + 2m_\pi}{m_\pi}\frac{T_\eta}{Q} - 1$, where where T_π denotes the kinetic energy of a given pion in the η rest frame, $Q = m_\eta - m_{\pi^+} - m_{\pi^-} - m_{\pi^0}$ is the excess energy of the reaction. The distributions of X and Y are shown in Fig. 1 (b) and (c). Using the same parameterization as in Ref. [12], the Dalitz plot parameters for $\eta \to \pi^+\pi^-\pi^0$ are determined to be $a = -1.128 \pm 0.015 \pm 0.008$, $b = \ \ 0.153 \pm 0.017 \pm 0.004$, $d = \ \ 0.085 \pm 0.016 \pm 0.009$, $f = \ \ 0.173 \pm 0.028 \pm 0.021$, which are in reasonable agreement with previous measurements.

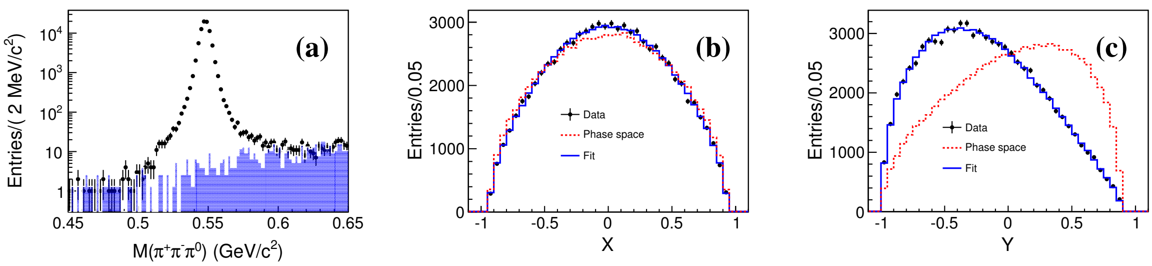

Figure 1: (a) Distribution of $\pi^+\pi^-\pi^0$ invariant mass. Projections of the Dalitz plot as a function of (b) X and (c) Y for $\eta \to \pi^+\pi^-\pi^0$ obtained from data (dots with error bars) and phase space distributed MC events (dashed line). The result of the fit described in the text (solid line) is also plotted.

Figure 2(a) shows the $\pi^0\pi^0\pi^0$ mass spectrum, where the η peak is quite clean and the background level is less than 1%. The distribution of the variable Z is displayed in Fig. 2(b). Due to the kinematic boundaries, the interval of $0 < Z < 0.7$, corresponding to the region of phase space where the Z distribution is flat, is used to extract the slope parameter α from the data. Analogous to the measurement for $\eta \to \pi^+\pi^-\pi^0$, an unbinned maximum likelihood fit, as displayed in the inset of Fig. 2(b), yields the Dalitz plot slope parameter $\alpha = -0.055 \pm 0.014 \pm 0.004$, which is compatible with the recent results from other experiments and in agreement with the prediction from ChPT at NNLO within two standard deviations of the theoretical uncertainties.

For $\eta' \to \pi^0\pi^0\pi^0$, the η' signal is also clearly observed in $\pi^0\pi^0\pi^0$ mass spectrum [Fig. 2(c)], where the hatched and shaded histogram show the background contributions estimated from the inclusive J/ψ decays and $\eta' \to \pi^0\pi^0\eta$, respectively. The Dalitz plot slope parameter for $\eta' \to \pi^0\pi^0\pi^0$ is measured to be $\alpha = -0.640 \pm 0.046 \pm 0.047$ [Fig. 2(d)], which is consistent with but more precise than previous measurements. The value deviates significantly from zero, which implies that final state interactions play an important role in the decay. Up to now, there are just a few predictions about the slope parameter of $\eta' \to \pi^0\pi^0\pi^0$. In Ref. [13], the slope parameter is predicted to be less than 0.03, which is excluded by our measurement.

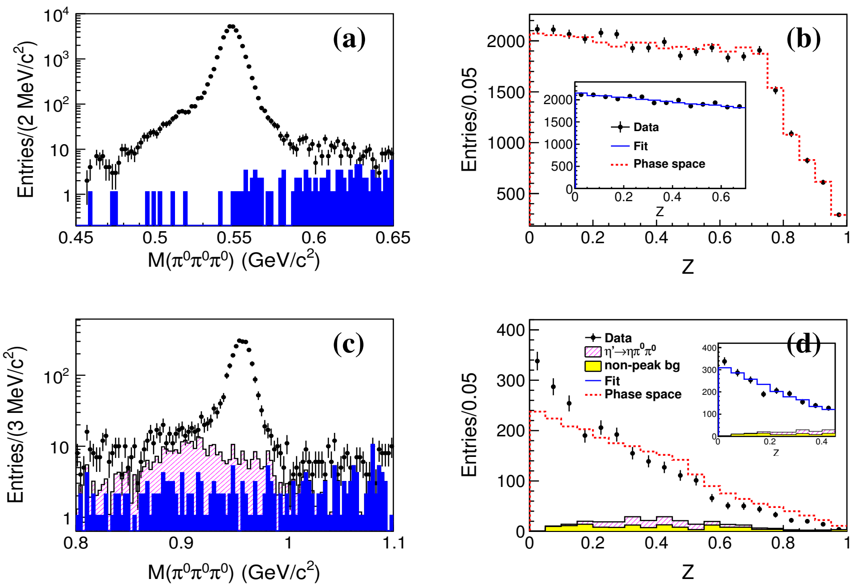

Figure 2: (a) Distribution of $\pi^0\pi^0\pi^0$ invariant mass. (b) Distribution of the kinematic variable Z for $\eta \to \pi^0\pi^0\pi^0$. (c) Distribution of $\pi^0\pi^0\pi^0$ invariant mass. (d) Distribution of the kinematic variable Z for $\eta' \to \pi^0\pi^0\pi^0$. Dots with error bars are for data, histograms for background contributions, dashed histograms for phase space distributed MC events and the solid lines in the inset are the results of the fit.

3. Observation of $\eta' \to \gamma e^+e^-$ [14]

Electromagnetic (EM) Dalitz decays of light pseudoscalar mesons, $P \to \gamma l^+l^-$ ($P = \pi^0$, η, η'; $l = e, \mu$), play an important role in revealing the structure of hadrons and the interaction mechanism between photons and hadrons [15]. In this work, we report the first observation of the Dalitz decay $\eta' \to \gamma e^+e^-$ as shown in Fig. 3 (a) and the branching fraction $\mathscr{B}(\eta' \to \gamma e^+e^-)$ is measured to be $(4.69 \pm 0.20 \pm 0.23) \times 10^{-4}$.

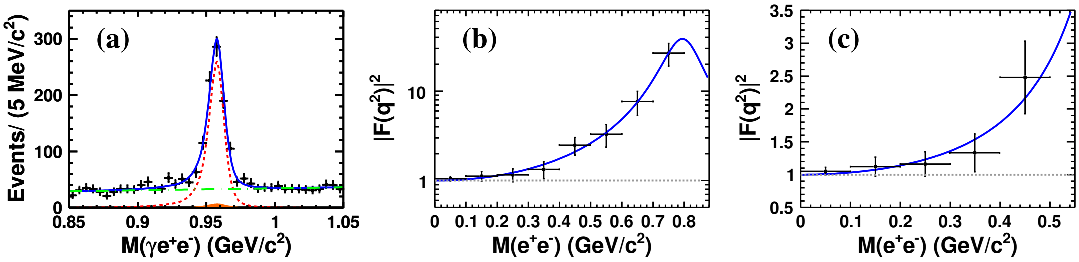

Figure 3: (a) Invariant γe^+e^- mass distribution for the selected signal events. The (black) crosses are the data, the (red) dashed line represents the signal, the (green) dot-dashed curve shows the non-peaking background shapes, the (orange) shaded component is the shape of the peaking background events. (b) Fit to the single pole form factor $|F|^2$. (c) Determination of the form factor slope by fitting to $|F|^2$.

In addition, we present measurements of the transition form factor (TFF) as a function of $M(e^+e^-)$ [Figs. 3 (b) and (c)], which could be described with a single pole parameterization of $F(q^2) = \frac{1}{(1-q^2/\Lambda^2)}$. The mass and width parameters of $\Lambda_{\eta'}$ and $\gamma_{\eta'}$ are determined to be $(0.79 \pm 0.04 \pm 0.02)$ GeV, and $\gamma_{\eta'} = (0.13 \pm 0.06 \pm 0.03)$ GeV, respectively. The slope of the TFF corresponds to $(1.60 \pm 0.17 \pm 0.08)$ GeV^{-2} and agrees within errors with the Vector Meson Dominance (VMD) model. predictions. The uncertainty of the η' transition form factor slope is in good agreement the best determination in the space-like region from the CELLO collaboration $b_{\eta'} = (1.60 \pm 0.16)$ GeV^{-2} [16], and improves the previous determination of the slope in the time-like region $b_{\eta'} = (1.7 \pm 0.4)$ GeV^{-2} [15, 17].

4. Observation of $\eta' \to \pi^+\pi^-\pi^+\pi^-, \pi^+\pi^-\pi^0\pi^0$ [18]

The hadronic decays $\eta' \to \pi^+\pi^-\pi^{+(0)}\pi^{-(0)}$ are not suppressed by approximate symmetries. Recently Guo, Kubis and Wirzba [19], using a combination of chiral perturbation theory (ChPT) and a vector-meson dominance (VMD) model, obtained the following prediction: $\mathscr{B}(\eta' \to \pi^+\pi^-\pi^+\pi^-) = (1.0 \pm 0.3) \times 10^{-4}$ and $\mathscr{B}(\eta' \to \pi^+\pi^-\pi^0\pi^0) = (2.4 \pm 0.7) \times 10^{-4}$. The $\pi^+\pi^-\pi^{+(0)}\pi^{-(0)}$ invariant mass distributions are shown in Figs. 4(a) and (b), respectively, where the η' peak is clearly seen. To ensure that the η' peak is not from background, an extensive MC study was performed. It was found, as displayed by the hatched histograms in Figs. 4(a) and (b), that none of these background sources produces a peak in the $\pi^+\pi^-\pi^+\pi^-$ invariant mass spectrum near the η' mass.

The signal yields are obtained from extended unbinned maximum likelihood fits to the $\pi^+\pi^-\pi^+\pi^-$ $\pi^+\pi^-\pi^0\pi^0$ and invariant mass distributions and the statistical significances for $\eta' \to \pi^+\pi^-\pi^+\pi^-$ and $\eta' \to \pi^+\pi^-\pi^0\pi^0$ are calculated to be 18σ and 5σ, respectively. The branching fractions of $\eta' \to \pi^+\pi^-\pi^{+(0)}\pi^{-(0)}$ are determined to be $\mathscr{B}(\eta' \to \pi^+\pi^-\pi^+\pi^-) = (8.53 \pm 0.69 \pm 0.64) \times 10^{-5}$ and $\mathscr{B}(\eta' \to \pi^+\pi^-\pi^0\pi^0) = (1.82 \pm 0.35 \pm 0.18) \times 10^{-4}$, which are consistent with the theoretical predictions based on a combination of chiral perturbation theory and vector-meson dominance [19], but not with the broken-$SU_6 \times O_3$ quark model [20].

5. Preliminary results: study of $\eta' \to \gamma\pi^+\pi^-$ decay dynamics

Theoretically the non-resonant part of coupling in $\eta' \to \gamma\pi^+\pi^-$ is accounted for by the higher

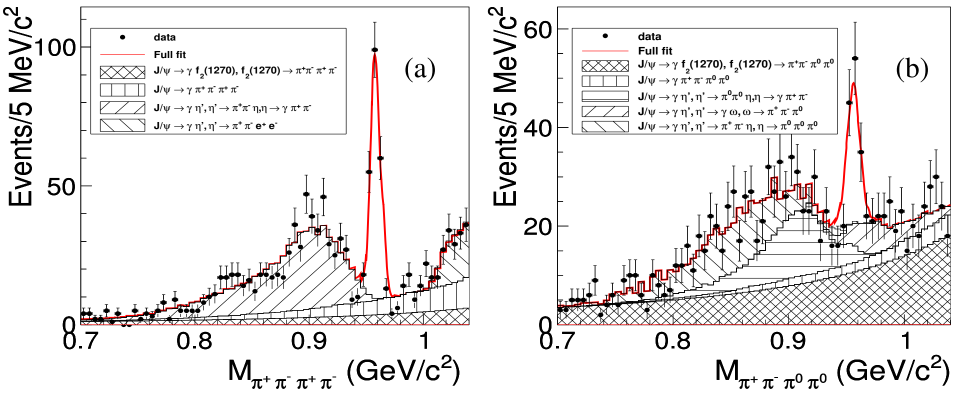

Figure 4: Results of the fits to (a) $M_{\pi^+\pi^-\pi^+\pi^-}$ and (b) $M_{\pi^+\pi^-\pi^0\pi^0}$, where the background contributions are displayed as the hatched histograms.

term of Wess-Zumino-Witten (WZW) ChPT Lagrangian[4] (also known as the box anomaly). However the decay dynamics of $\eta' \to \gamma\pi^+\pi^-$ has been explored with very limited statistics only and new measurements are needed to clarify the scenario. In this work, a sample of 9×10^5 $\eta' \to \gamma\pi^+\pi^-$ events is selected to investigate its decay dynamics and the $\pi^+\pi^-$ mass spectrum is shown in Fig. 5 with a background level of 1%.

The shape of the $M_{\pi^+\pi^-}$ spectrum is analyzed using parameterization relying on model-dependent and model-independent approaches respectively. For the model-dependent approach, the results show that only $\rho(770)$ resonance is insufficient to describe the data even if one takes into account both $\rho(770)$ and omega resonances and the interference between them. The fit performance gets much better after including the box anomaly [Fig. 5 (a)] with a statistical significance larger than 37σ. We also try to replace the box anomaly with $\rho(1450)$ [Fig. 5 (b)] by fixing its mass the width to be the world average values, the fit can also provide a reasonable description of data. Therefore, we conclude that in addition to $\rho(770)$ and ω, the box anomaly is necessary, but the contribution from $\rho(1450)$ could not be ruled out.

With the inclusion of ω into the expansion, $M_{\pi^+\pi^-}$ spectrum is very well described with the model-independent parameterisation [21] as shown in Fig. 5 (c), the values of parameters being $\alpha = 0.992 \pm 0.039 \pm 0.067$ GeV^{-2}, $\beta = -0.523 \pm 0.039 \pm 0.066$ GeV^{-4}, $\delta = 0.199 \pm 0.006 \pm 0.010$. The value of α found in this work is compatible with the work of [21].

6. Summary

In summary the recent results on η/η' decays at BESIII are presented with a sample of 1.3×10^8 J/ψ events. The Dalitz plots of $\eta\to\pi^+\pi^-\pi^0$ and $\eta/\eta'\to\pi^0\pi^0\pi^0$ are analyzed and the corresponding matrix elements are extracted; the new decay mode of $\eta'\to\gamma e^+e-$ is observed for the first time and the TFF is measured with the function of $M_{e^+e^-}$; the hadronic decays of $\eta'\to\pi^+\pi^-\pi^+\pi^-$ and $\eta'\to\pi^+\pi^-\pi^0\pi^0$ are also observed and the measurement branching fractions are consistent with the theoretical predictions; the decay dynamics of $\eta'\to\gamma\pi^+\pi^-$ is investigated with both model-dependent and model-independent parameterisations. It is found that the extra

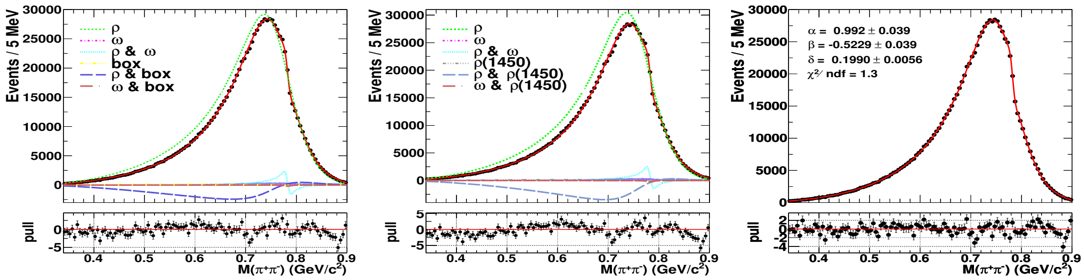

Figure 5: The results of the model-dependent fits to $M_{\pi\pi}$ with (a) $\rho - \omega -$ *box anomaly* and (b) $\rho - \omega - \rho(1450)$. (c) The results of model-independent fit with ω interference.

contribution is necessary to describe data besides the contributions from $\rho(770)$ and ω. The above results indicate that there is a rich field to be explored in η/η' physics, which motivates to search for their rare and forbidden decays.

References

[1] M. Ablikim *et al.* [BESIII Collaboration], Phys. Rev. D **92**, 012014 (2015).

[2] A. Anisovich and H. Leutwyler, Phys. Lett. B **375**, 335 (1996).

[3] S. P. Schneider, B. Kubis, and C. Ditsche, JHEP **1102**, 028 (2011).

[4] J. Gasser and H. Leutwyler, Nucl. Phys. B **250**, 539 (1985).

[5] J. Kambor, C. Wiesendanger and D. Wyler,Nucl. Phys. B **465**, 215 (1996).

[6] J. Bijnens and K. Ghorbani, JHEP **0711**, 030 (2007).

[7] K. Kampf, M. Knecht, J. Novotny and M. Zdrahal, Phys. Rev. D **84**, 114015 (2011).

[8] G. Colangelo, S. Lanz, H. Leutwyler and E. Passemar, PoS EPS **-HEP2011**, 304 (2011).

[9] P. Guo *et al.*, Phys. Rev. D **92**, 054016 (2015).

[10] H. Osborn and D. J. Wallace, Nucl. Phys. B **20**, 23 (1970); J. A. Cronin, Phys. Rev. **161**, 1483 (1967).

[11] K. A. Olive *et al.* [Particle Data Group], Chin. Phys. C **38**, 090001 (2014).

[12] F. Ambrosino *et al.* [KLOE Collaboration], JHEP **0805**, 006 (2008).

[13] C. Roiesnel, T. N. Truong, Paris Ec. Polytech. A **515**, 0982(1982).

[14] M. Ablikim *et al.* [BESIII Collaboration], Phys. Rev. D **83**, 012003 (2011).

[15] L. G. Landsberg, Phys. Rept. **128**, 301 (1985).

[16] H. J. Behrend *et al.* [CELLO Collaboration], Z. Phys. C **49**, 401 (1991).

[17] R. I. Dzhelyadin *et al.*, Phys. Lett. B **88**, 379 (1979).

[18] M. Ablikim *et al.* [BESIII Collaboration], Phys. Rev. Lett. **112**, 251801 (2014).

[19] Feng-Kun Guo, Bastian Kubis and Andreas Wirzba, Phys. Rev. D **85**, 014014 (2012).

[20] D. Parashar, Phys. Rev. D **19**, 268 (1979).

[21] F. Stollenwerk, C. Hanhart, A. Kupsc, U.-G. Meissner, A. Wirzba, Phys. Lett. B**707**, 184 (2012).